A Multi-lag Correlation Estimator for Polarimetric Radar Variables in the Presence of Noise

P13.25

Lei Lei[1, 3], Guifu Zhang[2, 3], Robert D. Palmer[2, 3], Boon Leng Cheong[3], Ming Xue[3, 4], and Qing Cao[1, 3]

[1]School of Electrical and Computer Engineering,
[2]School of Meteorology
[3]Atmospheric Radar Research Center (ARRC)
[4]Center for Analysis and Prediction of Storms (CAPS)
University of Oklahoma, Norman, Oklahoma

1. INTRODUCTION

In conventional autocovariance processing-the pulse pair processor (PPP), lag zero of auto-correlation function (ACF) and cross-correlation function (CCF) are used to estimate reflectivity, differential reflectivity and correlation coefficient; lag zero and one (or lag one and two) of ACF are used to estimate spectrum width. However, when signal-to-noise ratio (SNR) decreases, the quality of the polarimetric radar data degrades. To improve radar performance and data quality, a multi-lag correlation estimator is developed and examined in terms of moment estimation, where lag zero of the ACF is excluded to minimize noise effects. All useful lags of the ACF/CCF are used to estimate radar variables. This is based on the understanding that noise contributes mainly to lag zero of the auto-correlation function and noise effects can be minimized by fitting over other non-zero lags as used in wind estimation (Zhang *et al.*, 2004).

A multi-lag technique is presented to estimate radar reflectivity, spectrum width, differential reflectivity, and correlation coefficient. Biases and standard deviations of the multi-lag estimates are calculated and compared with those of the conventional PPP. Theoretical analysis of the estimation errors are provided and verified by numerical simulations.

2. MULTI-LAG ESTIMATORS

The conventional estimator calculates power from the lag zero of the ACF. However, lag zero of ACF contains noise power. To minimize noise effects, a multi-lag estimator derives radar moments using correlation estimates at other lags: $\hat{C}(T_s)$, $\hat{C}(2T_s)$, $\hat{C}(3T_s)$, $\hat{C}(4T_s)$ …etc. (C is the ACF).

*Corresponding author address: Lei Lei, 120 David L. Boren Blvd. Suite 5310, Univ. of Oklahoma, Norman, OK, 73072, U.S.A; e-mail: leilei@ou.edu

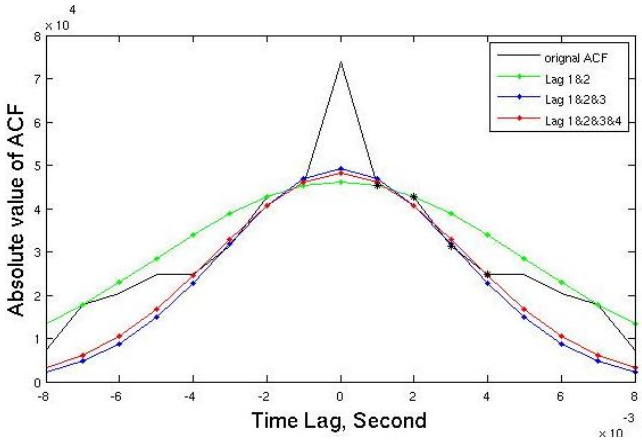

Figure 1: An example of multi-lag estimations. Lag 1&2 (green), lag 1&2&3 (blue) and lag 1&2&3&4 (red) estimates of ACF data (black) are used to fit a Gaussian function estimate of the expected ACF.

Figure 1 shows an example of multi-lag estimations for ACF. The black line denotes the absolute value of the ACF data, where the impulse at zero lag is caused by noise. The multi-lag estimator uses the ACF estimates to fit a Gaussian function at multi-lags: two-lags (green line), three-lags (blue line), and four-lags (red line). The fitted Gaussian function(s) is then used to calculate radar moments instead of the noise-contaminated ACF datum at zero lag.

The expected ACF and CCF have the Gaussian form.

$$C_H(nT_s) = S_H \rho(nT_s) \exp(-\frac{j\pi n v_H}{v_a}) + N_H \delta_{m,0} \qquad (1)$$

$$C_{HV}(nT_s) = \sqrt{S_H S_V}\, \rho_{hv} \rho(nT_s) \cdot \exp(-\frac{j\pi n v_{HV}}{v_a} + j\varphi_{dp}) \qquad (2)$$

where, S_H , S_V are the signal powers from the H or V channel, respectively. $\rho(nT_s) = \exp(-\frac{\tau^2}{2\tau_c^{\,2}})$, $\tau_c = \frac{\lambda}{4\pi\sigma_v}$,

v_a is the Nyquist velocity. N_H is the expected value of white noise power from the H channel, and v_H is radial velocity associated with hydrometeors backscattering signals to the H channel. We assume $v_{HV} = v_H = v_V$. φ_{dp} is differential phase, ρ_{hv} is correlation coefficient, T_s is pulse repetition time,

The ACF and CCF are estimated from time-series data by

$$\hat{C}_H(nT_s) = \frac{1}{M-|n|}\sum_{m=1}^{M-|n|} E_m^{(h)} \cdot E_{m+n}^{(h)*} \tag{3}$$

$$\hat{C}_{HV}(nT_s) = \frac{1}{M-|n|}\sum_{m=1}^{M-|n|} E_m^{(h)} \cdot E_{m+n}^{(v)*} \tag{4}$$

where, M is the number of samples, $E_m^{(h)}$ is voltage of horizontal channel. $E_m^{(v)}$ is voltage of vertical channel.

2.1 Lag 1-2 estimator

Using ACF estimates at lag 1 and lag 2: $\hat{C}(T_s)$ and $\hat{C}(2T_s)$ power and CCF estimate at lag zero, radar variables of spectrum width, differential reflectivity and correlation coefficient are estimated as

$$\hat{S}_H = \frac{|\hat{C}_H(T_s)|^{\frac{4}{3}}}{|\hat{C}_H(2T_s)|^{\frac{1}{3}}} \tag{5}$$

$$\hat{\sigma}_v = \frac{\lambda}{\sqrt{24}\pi T_s}\cdot\sqrt{ln|\hat{C}_H(T_s)| - ln|\hat{C}_H(2T_s)|} \tag{6}$$

$$\hat{Z}_{DR} = 10\log_{10}\left(\frac{|\hat{C}_H(T_s)|^{\frac{4}{3}}}{|\hat{C}_H(2T_s)|^{\frac{1}{3}}}\cdot\frac{|\hat{C}_V(2T_s)|^{\frac{1}{3}}}{|\hat{C}_V(T_s)|^{\frac{4}{3}}}\right) \tag{7}$$

$$\hat{\rho}_{hv} = \hat{C}_{HV\_fit}(0)\cdot\frac{|\hat{C}_H(2T_s)|^{\frac{1}{6}}\cdot|\hat{C}_V(2T_s)|^{\frac{1}{6}}}{|\hat{C}_H(T_s)|^{\frac{2}{3}}\cdot|\hat{C}_V(T_s)|^{\frac{2}{3}}} \tag{8}$$

where $\hat{C}_{HV\_fit}(0)$ is fitted value of CCF estimates over lag 0, lag ±1, and lag ±2 because its absolute value is not symmetric.

2.2 Lag 1-3 estimator

The lag 1-3 estimator is to estimate radar variables using ACF and CCF estimates at lag 1, lag 2, and lag 3. The correlation estimaes $\hat{C}(T_s)$ $\hat{C}(2T_s)$ and $\hat{C}(3T_s)$ are least square-fitted to the Gaussian function.

Taking the natural logarithm of both sides of Eq. (1), the true value of ACF is expressed by:

$$\ln(|C_H(nT_s)|) = an^2T_s^2 + b, \tag{9}$$

where: $-\frac{1}{2\tau_c^2} = a$, $ln(S_H) = b$,

and rewrite these compactly: $ln(|\hat{C}_H(T_s)|) = y_1$,

$ln(|\hat{C}_H(2T_s)|) = y_2$, $ln(|\hat{C}_H(3T_s)|) = y_3$

Using Eq. (9) to form the least square function $F(a,b)$:

$$F(a,b) = (aT_s^2 + b - \hat{y}_1)^2 + (4aT_s^2 + b - \hat{y}_2)^2 + (9aT_s^2 + b - \hat{y}_3)^2 \tag{10}$$

When the Eq. (10) reaches its smallest value, we have equations:

$$\begin{cases}\dfrac{\partial F(a,b)}{\partial a} = 0\\ \dfrac{\partial F(a,b)}{\partial b} = 0\end{cases}$$

and solve them for *a* and *b*. Hence, arrive at:

$$\begin{cases}\hat{S}_H = \dfrac{|\hat{C}_H(T_s)|^{\frac{6}{7}}\cdot|\hat{C}_H(2T_s)|^{\frac{3}{7}}}{|\hat{C}_H(3T_s)|^{\frac{2}{7}}}\\ \hat{\sigma}_v = \dfrac{\lambda}{28\pi T_s}\cdot\sqrt{11\cdot ln|\hat{C}_H(T_s)| + 2\cdot ln|\hat{C}_H(2T_s)| - 13\cdot ln|\hat{C}_H(3T_s)|}\end{cases} \tag{11}$$

Further, we obtain differential reflectivity and correlation coefficient using the result of Eq. (11) as follows:

$$\hat{Z}_{DR} = 10\log_{10}\left(\frac{|\hat{C}_H(T_s)|^{\frac{6}{7}}\cdot|\hat{C}_H(2T_s)|^{\frac{3}{7}}}{|\hat{C}_H(3T_s)|^{\frac{2}{7}}}\cdot\frac{|\hat{C}_V(3T_s)|^{\frac{2}{7}}}{|\hat{C}_V(T_s)|^{\frac{6}{7}}\cdot|\hat{C}_V(2T_s)|^{\frac{3}{7}}}\right)$$

$$\hat{\rho}_{hv} = \hat{C}_{HV\_fit}(0)\cdot\frac{|\hat{C}_H(3T_s)|^{\frac{1}{7}}\cdot|\hat{C}_V(3T_s)|^{\frac{1}{7}}}{|\hat{C}_H(T_s)|^{\frac{3}{7}}\cdot|\hat{C}_H(2T_s)|^{\frac{3}{14}}\cdot|\hat{C}_V(T_s)|^{\frac{3}{7}}\cdot|\hat{C}_V(2T_s)|^{\frac{3}{14}}} \tag{12}$$

2.3 Lag 1-4 estimator

In the same approach to derive the lag 1-3 estimator, the lag 1-4 estimators can be developed as:

$$\hat{S}_H = \frac{|\hat{C}_H(T_s)|^{\frac{54}{86}}\cdot|\hat{C}_H(2T_s)|^{\frac{39}{86}}\cdot|\hat{C}_H(3T_s)|^{\frac{14}{86}}}{|\hat{C}_H(4T_s)|^{\frac{21}{86}}}$$

$$\hat{\sigma}_v = \frac{\lambda}{4\sqrt{129}\pi T_s}\cdot\sqrt{13\cdot ln|\hat{C}_H(T_s)| + 7\cdot ln|\hat{C}_H(2T_s)| - 3\cdot ln|\hat{C}_H(3T_s)| - 17\cdot ln|\hat{C}_H(4T_s)|}$$

$$\hat{Z}_{DR} = 10\log_{10}\left(\frac{|\hat{C}_H(T_s)|^{\frac{54}{86}} \cdot |\hat{C}_H(2T_s)|^{\frac{39}{86}} \cdot |\hat{C}_H(3T_s)|^{\frac{14}{86}}}{|\hat{C}_H(4T_s)|^{\frac{21}{86}}} \cdot \frac{|\hat{C}_V(4T_s)|^{\frac{21}{86}}}{|\hat{C}_V(T_s)|^{\frac{54}{86}} \cdot |\hat{C}_V(2T_s)|^{\frac{39}{86}} \cdot |\hat{C}_V(3T_s)|^{\frac{14}{86}}} \right)$$

$$\hat{\rho}_{hv} = \hat{C}_{HV\_fit}(0) \cdot \frac{|\hat{C}_H(4T_s)|^{\frac{21}{172}} \cdot |\hat{C}_V(4T_s)|^{\frac{21}{173}}}{|\hat{C}_H(T_s)|^{\frac{27}{86}} \cdot |\hat{C}_H(2T_s)|^{\frac{39}{172}} \cdot |\hat{C}_H(3T_s)|^{\frac{7}{86}}} \cdot \frac{1}{|\hat{C}_V(T_s)|^{\frac{27}{86}} \cdot |\hat{C}_V(2T_s)|^{\frac{39}{172}} \cdot |\hat{C}_V(3T_s)|^{\frac{7}{86}}}$$

3. PERFORMANCE OF THE ESTIMATORS

In this section, performance of the multi-lag estimators are examined through error analysis and compared with that of the conventional estimators. The detailed error analysis can be found in Lei (2009). Theoretical biases and standard deviations of **power**, **spectrum width**, **differential reflectivity** estimates are calculated and verified by simulations.

3.1 Signal power

For the conventional estimator Eq. (13), bias comes from accuracy of noise level estimation. The noise level estimation depends on the noise types (Fang *et al.* 2004). Due to the changes of the expected noise power or because the estimated noise power deviates from true noise power, the conventional estimator does not perform well at low SNR. A multi-lag estimator is an efficient way to resolve this problem.

Four power estimators of conventional, lag 1, lag 1-2, and lag 1-4 are expressed as:

$$\hat{S}_H = \hat{C}_H(0) - \hat{N}_H \tag{13}$$

$$\hat{S}_H = |\hat{C}_H(T_s)| \tag{14}$$

$$\hat{S}_H = \frac{|\hat{C}_H(T_s)|^{\frac{4}{3}}}{|\hat{C}_H(2T_s)|^{\frac{1}{3}}} \tag{15}$$

$$\hat{S}_H = \frac{|\hat{C}_H(T_s)|^{\frac{54}{86}} \cdot |\hat{C}_H(2T_s)|^{\frac{39}{86}} \cdot |\hat{C}_H(3T_s)|^{\frac{14}{86}}}{|\hat{C}_H(4T_s)|^{\frac{21}{86}}} \tag{16}$$

We ignore lag 1-3 estimator because its performance is between that of lag 1-2 and that of lag 1-4. Biases of power estimates using different estimators are shown in Figure 2. The calculations can be found in Lei (2009).

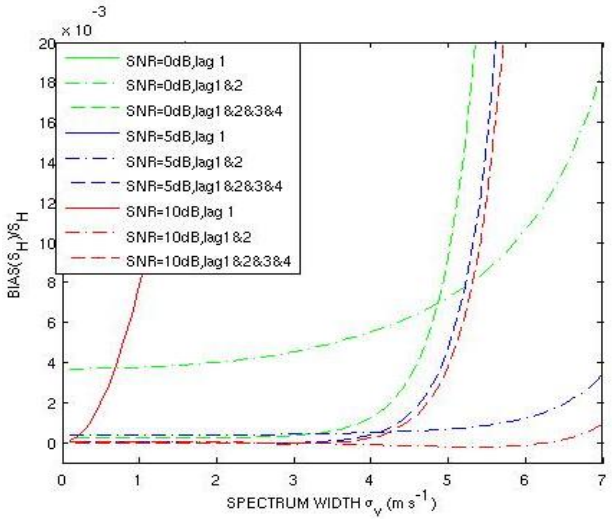

Figure 2: Bias of power estimation, M = 128, $T_s = 0.001s$: Green is SNR=0 dB, blue is SNR=5dB, red is SNR=10dB. For the lag 1, three lines are overlapped.

The bias is the function of SNR, M (number of samples) and spectrum width. Increasing of M and SNR will decrease the bias. As expected, the biases increase as SNR decreases. Lag 1 estimator is a biased estimator and has the largest bias among these estimators. Lag 1-4 estimator has less bias than lag 1-2 estimator at spectrum width less than 3.5 m/s and if the SNR is less than 10 dB.

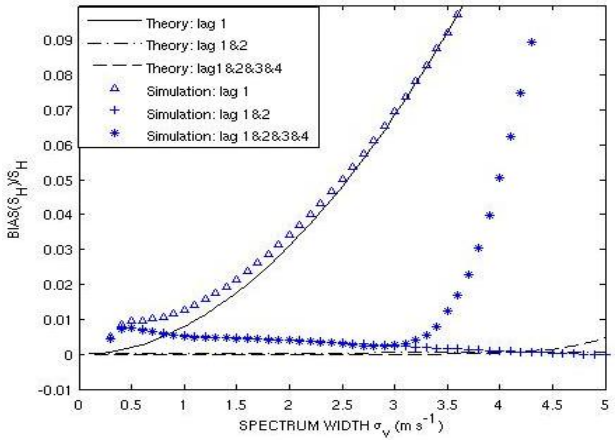

Figure 3: Comparison between theory and simulations of power biases. SNR=5 dB, M=128, $T_s = 0.001s$

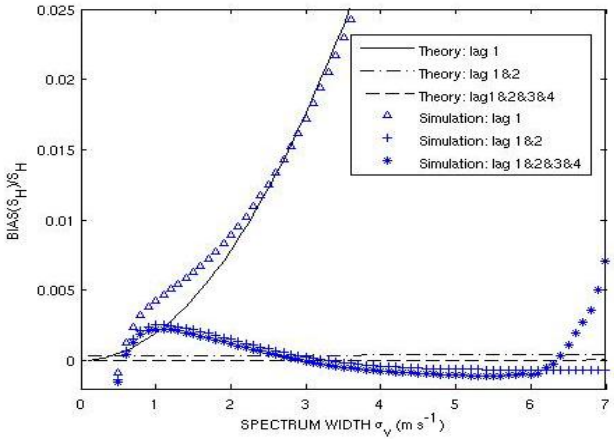

Figure 4: Comparison between theory and simulations of power biases. Only change T_s to half of the value in the previous Figure 3. SNR=5 dB, M = 128 , $T_s = 0.0005s$

The theoretical analysis is verified with simulations where dual-polarzation radar signals are generated using a spectrum method (Zrnic, 1975; Galati *et al*, 1995). The results are shown in Figure 3 and 4. For the lags 1-4 estimator, the analytical results and simulations differ when the spectrum width is larger than 3.5 m/s. This is caused by the under sampling rate at larger spectrum width. By decreasing the PRT, as shown in Figure 4, the difference between theory and simulation diminished significantly. In the calculation of bias and standard deviation, we use the Taylor expansion which is only valid when the estimated value is very near the true value. So the theory results will be true only when the bias and standard deviation is not large (within 10% of the true value). When the pulse number or SNR is increasing to reduce the bias and standard deviation, the theory will match simulation better.

Standard deviation of power is shown in Figure 5 and Figure 6.

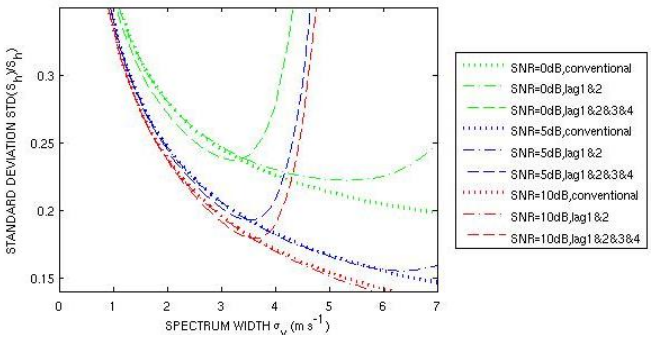

Figure 5: Standard deviation of signal power, M = 128, $T_s = 0.001s$, Green is SNR=0 dB, blue is SNR=5dB, red is SNR=10dB.

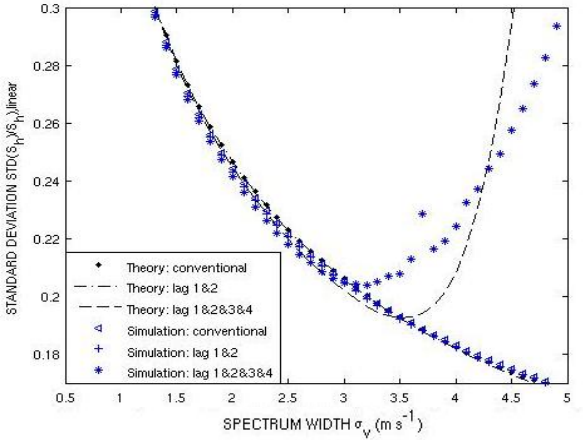

Figure 6: Comparison between theory and simulations of power standard deviations. SNR=5dB, M=128, $T_s = 0.001s$

The conventional estimator calculated here assumes the noise level is accurately estimated. If not, the bias of conventional estimator will be larger than the results shown in the figures. Taking both bias and variance into consideration, lag 1-4 estimator is the best estimator when the SNR is under 10 dB and the spectrum width is less than 3.5m/s with the given radar parameters. However, multi-lag estimator is not performing well on large spectrum width. Lag 1-2 estimator has large standard deviation when SNR is low as we expected from the Eq. (15).

3.2 Spectrum width

Four spectrum width estimators: conventional (lag 0 and 1), lag 1- 2, lag 1-3, lags 1-4, are expressed, respectively, by

$$\hat{\sigma}_v = \frac{\lambda}{2\pi T_s\sqrt{2}}\sqrt{ln(|\hat{S}|) - ln(|\hat{C}_H(T_S)|)}$$

$$\hat{\sigma}_v = \frac{\lambda}{\sqrt{24}\pi T_s}\cdot\sqrt{ln|\hat{C}_H(T_s)| - ln|\hat{C}_H(2T_s)|}$$

$$\hat{\sigma}_v = \frac{\lambda}{28\pi T_s}\cdot\sqrt{\begin{matrix}11\cdot ln|\hat{C}_H(T_s)| + 2\cdot ln|\hat{C}_H(2T_s)| \\ -13\cdot ln|\hat{C}_H(3T_s)|\end{matrix}}$$

$$\hat{\sigma}_v = \frac{\lambda}{4\sqrt{129}\pi T_s}\cdot\sqrt{\begin{matrix}13\cdot ln|\hat{C}_H(T_s)| + 7\cdot ln|\hat{C}_H(2T_s)| \\ -3\cdot ln|\hat{C}_H(3T_s)| - 17\cdot ln|\hat{C}_H(4T_s)|\end{matrix}}$$

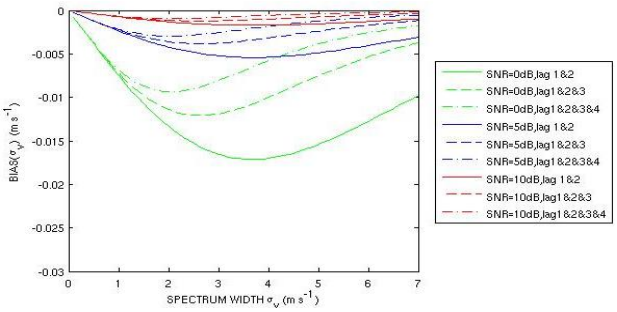

Figure 7: Bias of spectrum width, M = 128, $T_s = 0.001s$. Green is SNR=0 dB; Blue is SNR=5dB; Red is SNR=10dB.

The biases of spectrum width of the estimators are compared in Figure 7. When the SNR is small, the bias becomes larger. Under certain SNR and radar parameters, the more lags used to fit, the less the bias of the spectrum width.

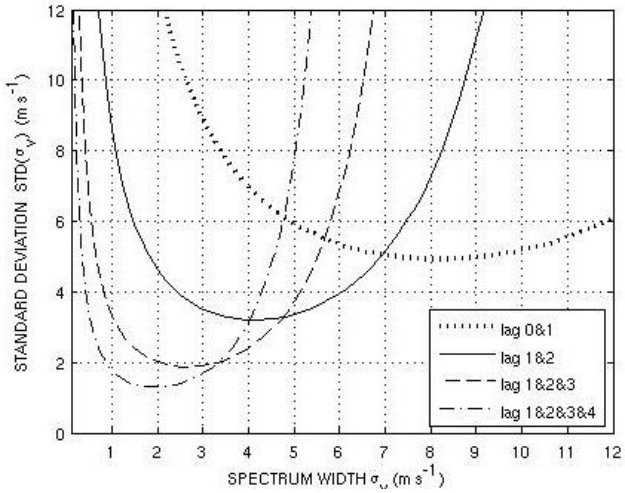

Figure 8: Standard deviation of spectrum width. SNR = -5dB, M =64, $T_s = 0.001s$. Lag 0&1, lag 1-2, lag 1-3, lag 1-4 are compared.

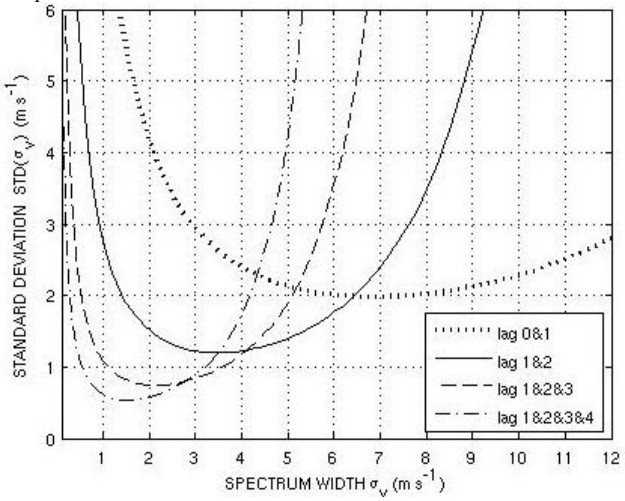

Figure 9: Standard deviation of spectrum width. SNR = 0dB, other parameters are the same as the previous Figure 8.

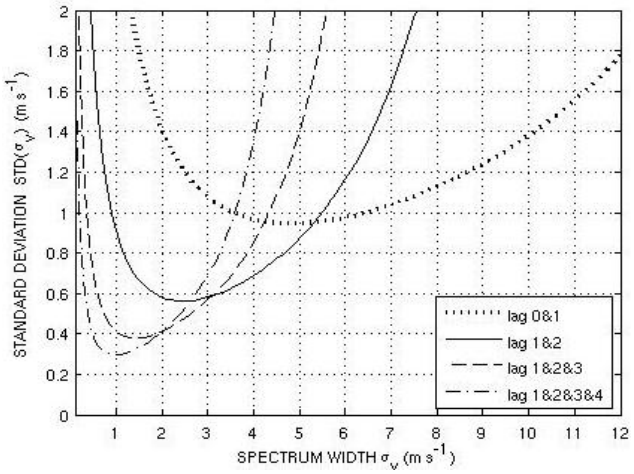

Figure 10: Standard deviation of spectrum width, SNR=5dB, other parameters are the same as the previous Figure 9.

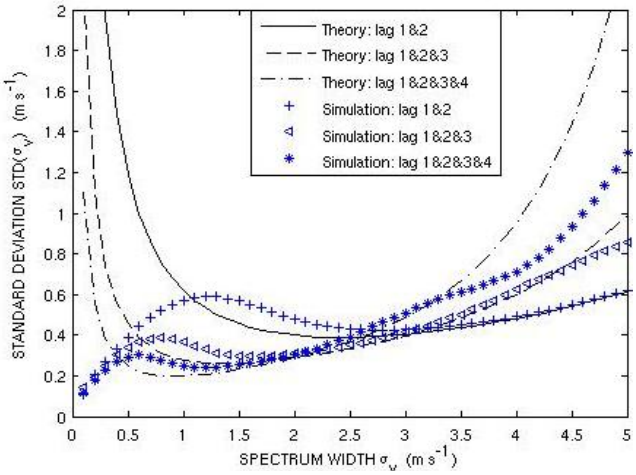

Figure 11: Comparison between theory and simulations of spectrum width standard deviations.SNR=5 dB, M = 128, $T_s = 0.001s$

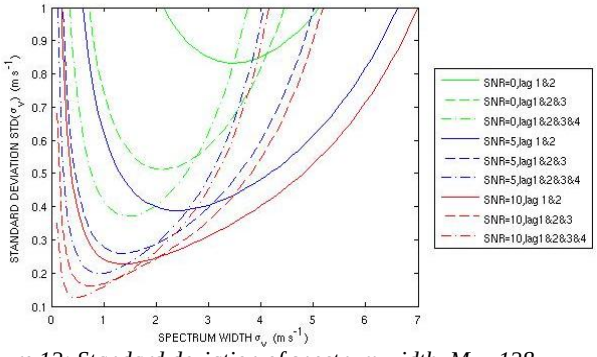

Figure 12: Standard deviation of spectrum width. M = 128 , $T_s = 0.001s$. Green is SNR=0 dB, blue is SNR=5dB, red is SNR=10dB.

From Figure 7 to Figure 12, the more lags we use, the better results are shown in bias and standard deviation when the spectrum width is small. However as the

spectrum width is large, the multi-lag fitting method has poorer performance than the conventional estimator in standard deviation.

3.3 Differential reflectivity

The differential reflectivity is a ratio of the reflected horizontal and vertical power returns. Four estimators: conventional (lag 0), lag 1, lag 1-2, and lag 1-4 are examined.

$$\hat{Z}_{DR} = 10\log_{10}\left(\frac{\hat{S}_H}{\hat{S}_V}\right)$$

$$\hat{Z}_{DR} = 10\log_{10}\left(\frac{|\hat{C}_H(T_s)|}{|\hat{C}_V(T_s)|}\right)$$

$$\hat{Z}_{DR} = 10\log_{10}\left(\frac{|\hat{C}_H(T_s)|^{\frac{4}{3}}}{|\hat{C}_H(2T_s)|^{\frac{1}{3}}}\cdot\frac{|\hat{C}_V(2T_s)|^{\frac{1}{3}}}{|\hat{C}_V(T_s)|^{\frac{4}{3}}}\right)$$

$$\hat{Z}_{DR} = 10\log_{10}\left(\frac{|\hat{C}_H(T_s)|^{\frac{54}{86}}\cdot|\hat{C}_H(2T_s)|^{\frac{39}{86}}\cdot|\hat{C}_H(3T_s)|^{\frac{14}{86}}}{|\hat{C}_H(4T_s)|^{\frac{21}{86}}}\cdot\frac{|\hat{C}_V(4T_s)|^{\frac{21}{86}}}{|\hat{C}_V(T_s)|^{\frac{54}{86}}\cdot|\hat{C}_V(2T_s)|^{\frac{39}{86}}\cdot|\hat{C}_V(3T_s)|^{\frac{14}{86}}}\right)$$

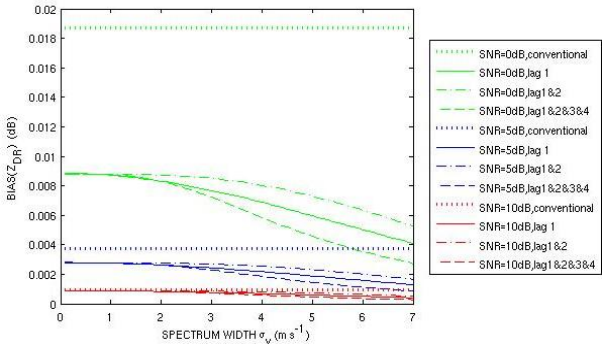

Figure 13: Bias of differential reflectivity, M = 128, $\rho_{hv} = 0.97$, $Z_{DR} = 1dB$, $T_s = 0.001s$ Green is SNR=0 dB, blue is SNR=5dB, red is SNR=10dB.

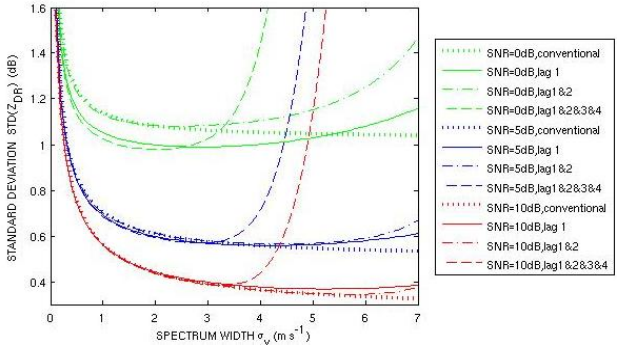

Figure 14: Standard deviation of differential reflectivity. M =128, $\rho_{hv} = 0.97$, $Z_{DR} = 1dB$, $T_s = 0.001s$. Green is SNR=0 dB, blue is SNR=5dB, red is SNR=10dB. Conventional, lag 1, lag 1-2, lag 1-4 estimators are compared.

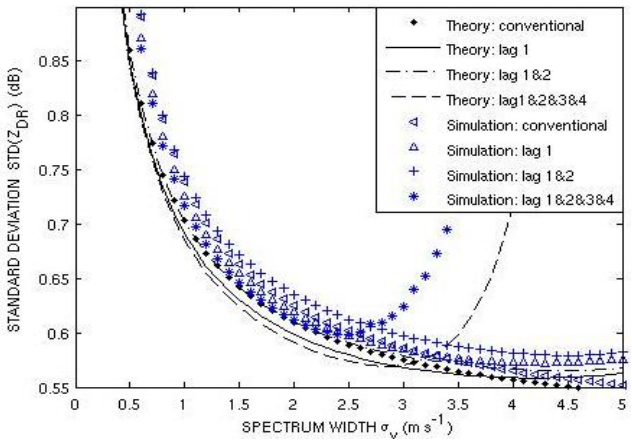

Figure 15: Comparison between theory and simulations of differential reflectivity standard deviations.SNR=5 dB, M=128, $\rho_{hv} = 0.97$, $Z_{DR} = 1dB$, $T_s = 0.001s$

The conventional estimator calculated here is assuming that the noise level is accurately estimated. If not, the bias of conventional estimator will be larger than the results shown in the figures. From Figure 13 and Figure 14, multi-lag method outperforms conventional method in both bias and standard deviation with small spectrum width. Comparing lag 1-4 estimator with lag 1 estimator, the former one is better than latter one in bias for the whole region, however it only performs better at small spectrum width region for standard deviation.

3.4 Correlation coefficient

Correlation Coefficient is the statistical correlation between the reflected horizontal and vertical power returns. We use both auto ACF and CCF to estimate correlation coefficient. For the auto correlation function, lag 1,2,3,4… are used to estimate; for the cross

correlation,…-3, -2, -1, 0, 1, 2, 3… are used to estimate.

Here are the lists of four types of estimators: conventional (lag 0), lag 1, lag 1-2, lag 1-4, respectively.

$$\hat{\rho}_{hv} = \frac{\hat{C}_{HV}(0)}{(\hat{S}_H \cdot \hat{S}_V)^{1/2}}$$

$$\hat{\rho}_{hv} = \frac{|\hat{C}_{HV}(T_s)|}{(|\hat{C}_H(T_s)| \cdot |\hat{C}_V(T_s)|)^{1/2}}$$

$$\hat{\rho}_{hv} = \hat{C}_{HV\_fit}(0) \cdot \frac{|\hat{C}_H(2T_s)|^{\frac{1}{6}} \cdot |\hat{C}_V(2T_s)|^{\frac{1}{6}}}{|\hat{C}_H(T_s)|^{\frac{2}{3}} \cdot |\hat{C}_V(T_s)|^{\frac{2}{3}}}$$

$$\hat{\rho}_{hv} = \hat{C}_{HV\_fit}(0) \cdot \frac{|\hat{C}_H(4T_s)|^{\frac{21}{172}} \cdot |\hat{C}_V(4T_s)|^{\frac{21}{173}}}{|\hat{C}_H(T_s)|^{\frac{27}{86}} \cdot |\hat{C}_H(2T_s)|^{\frac{39}{172}} \cdot |\hat{C}_H(3T_s)|^{\frac{7}{86}}} \cdot \frac{1}{|\hat{C}_V(T_s)|^{\frac{27}{86}} \cdot |\hat{C}_V(2T_s)|^{\frac{39}{172}} \cdot |\hat{C}_V(3T_s)|^{\frac{7}{86}}}$$

Where, $\hat{C}_{HV\_fit}(0)$ can use … -3 -2 -1 0 1 2 3… lags to fit. Because the cross-correlation is not symmetric and lag zero is not affected by noise. So more lags can be used to estimate $\hat{C}_{HV}(0)$ compared to auto correlation function.

4. SUMMARY

A multi-lag estimator has been developed to improve the estimation of polarimetric radar data in the presence of noise. It is possible to produce meaningful polarimetric radar measurements of weak echoes such as clouds and drizzle using the multi-lag estimator. The multi-lag estimator produces moment estimates with smaller bias and standard deviation than conventional estimators when the spectrum width is small.

In this study, equal weights have been used in Gaussian fitting to derive the multi-lag estimator. In practice, weights should be dependent on the merit and reliability of the estimates. It is expected that variable weights and adjustable number of lags would produce even more accurate estimates. Hence, an adaptive estimator will be developed, which can automatically choose how many lags to use and how to weight them according to the spectrum width and SNR.

REFERENCES:

Doviak, R.J., and D. S. Zrnić, 1993: Doppler Radar and Weather Observations. 2nd ed. Academic Press, 154-156.

Fang, M., R. J. Doviak, and V. Melnikov, 2004: Spectrum Width measured by WSR-88D radar. *J.Atmos.Oceanic Technol*. **21**, 888-904.

Galati G., and Pavan G., 1995: Computer Simulation of Weather Radar Signals. *Simul. Pr. Theory* **, 3**, 17-44.

Lei Lei, 2009: Simulation and Processing of Polarimetric Radar Signals Based on Numerical Weather Prediction Model output. Master thesis. University of Oklahoma.

May, P. T. , 1988: Statistical errors in the determination of wind velocities by the Spaced Antenna technique. *J. Atmos. And Terr. Phys*. **50**, 21-32.

Melnikov, V.M., and D.S., Zrnić, 2004: Simultaneous transmission mode for the Polarimetric WSR-88D: Statistical biases and standard deviations of polarimetric variables. NOAA/NSSL Rep., 1-84.

Melnikov, V.M., and D.S., Zrnić, 2007: Autocorrelation and Cross-Correlation estimators of Polarimetric variables. *Amer. Meteor. Soc.,* **24**, 1337-1350

Zhang, G., L. Tsang, and Y. Kuga, 1998, Numerical studies of the Detection of Targets in Clutter by using Angular Correlation Function and Angular Correlation Imaging, *Microwave and Optical Technology Letters*, **17**, 82-86

Zhang, G., Doviak, R.J., J. Vivekanandan, Brown, W.O.J., and Cohn, S.A., 2003: Cross-correlation ratio method to estimate Cross-beam Wind and comparison with a Full Correlation Analysis. *Radio Sci***., 38**, 8052

Zhang, G., Doviak, R.J., and J. Vivekanandan, 2004: Performance of correlation estimators for Spaced-Antenna Wind measurement in the presence of Noise. *Radio Sci*., **39**, 3017.

Zhang, G., Palmer, R. D., and Cao, Q., 2009: Survey and Assessment of relevant Radar Technologies. unpublished.

Zrnić, D. S., 1975: Simulation of weatherlike Doppler spectra and signals. *J. Appl. Meteor.*, **14**, 619-620.

Zrnić, D. S., 1979: Spectrum width Estimates for weather echoes. *IEEE Trans. Aerosp. Electron. Syst.* **15**, 613-619